The Dynamics of Cadmium Telluride Etching

K. D. Dobson, P. D. Paulson, B. E. McCandless and R. W. Birkmire
Institute of Energy Conversion, University of Delaware, Newark, DE 19716 USA

ABSTRACT

CdTe etching was investigated using variable angle spectroscopic ellipsometry and glancing angle x-ray diffraction. Treatment with HNO_3:H_3PO_4 (NP) based etches was shown to form amorphous-Te surface films which spontaneously crystallize following etching. Br_2/methanol (BM) etching forms very thin amorphous-Te films. NP-etched surfaces are stable in ambient air for ~1 hr before beginning to oxidize, while BM etched films oxidize immediately following treatment. CdTe grain boundary etching by NP was minimized using more acidic etches. Device analysis suggests that a higher Te content produces more stable back contacts by attenuating Cu diffusion. Mechanistic details of NP etching are discussed.

INTRODUCTION

Wet chemical etching is used in a number of technologies and industries in order to achieve contaminant-free material surfaces. A critical aspect of back contact processing for CdTe/CdS cells is the preparation of a Te-rich CdTe surface to allow the formation of back contacts on reaction with metals. Most research groups utilize an oxidizing wet chemical etch to form Te-rich CdTe surfaces. Wet etches allow fast treatment times and are easy to use. Only small solution volumes are generally used and often no heating of the solution or substrate is required. However, penetration of etchants into the cell structure, the action of the atmosphere on the freshly etched surface and changes to film and grain boundary (GB) morphology during etching may affect device performance.

Currently, two oxidizing etches are popularly employed for CdTe/CdS contacting at a research level; aqueous HNO_3/H_3PO_4 (NP) and Br_2/methanol (BM). It is understood that these treatments do indeed produce Te-rich CdTe surfaces [1-3], however, despite their widespread use, the action of these etches on the CdTe surface is not completely understood. A knowledge of etchant behavior and the nature of the CdTe surface throughout the reaction, including its reactivity towards the atmosphere and back contact metals, will allow optimization of wet chemical treatments to form stable back contacts to CdTe/CdS cells. Generally the etch solutions are corrosive and toxic, therefore the development of a universal and safe wet etchant that can be easily applied to CdTe films, independent of thickness and history, would be advantageous for scale-up of the CdTe device processing. In this paper the action of various NP and BM etches on CdTe films has been investigated. Effects of concentration, acidity, and solution viscosity were studied, with the aim of understanding the mechanistic details of the etch process and to develop an optimized wet chemical etch for CdTe contact processing. Variable angle spectroscopic ellipsometry (VASE) and glancing angle x-ray diffraction (GIXRD), techniques that are sensitive to surface changes, were employed to monitor the effects of CdTe etching. These effects were correlated with device performance.

EXPERIMENTAL

All measurements were carried out on 5 μm CdTe films deposited on ITO/7059 glass substrates. NP etch solutions were prepared with concentrated acids, 70% HNO_3 and 85% H_3PO_4. A series of NP etch solutions, 1:70:29 by vol. HNO_3:H_3PO_4:H_2O (NP1), 1:99:0 by vol. HNO_3:H_3PO_4:H_2O (NP2) and 0.5:99.5:0 by vol. HNO_3:H_3PO_4:H_2O (NP3), were used. NP etch solutions are stable during storage for many months. BM etches containing 0.01 – 0.1%, Br_2 were used for CdTe etching. Br_2 solutions can expire within less than a day due to reaction of Br_2 with the solvent and vapor loss. Therefore, Br_2 solutions were always prepared immediately prior to use. During NP and BM etching, samples were completely immersed in the etch solution for the required time. Upon removal, films were immediately washed with distilled water and dried with an Ar(g) flow. Samples were then immediately transferred for measurement. All measurements were begun within 2-3 minutes of etching

Scanning ellipsometry measurements were carried out using a J.A. Woollam VASE. The VASE is a rotating analyzer ellipsometer equipped with an auto-retarder. Measurements were carried out at room temperature with the sample under Ar(g) flow to reduce surface oxidation, unless otherwise stated. Spectra were recorded at 65 – 75° incident angles to bracket the Brewster angle for Te and CdTe. GIXRD measurements were carried out using a Rigaku D/Max 2100 x-ray diffractometer in asymmetric mode with parallel beam geometry at 40 kV CuK_α. Scanning electron microscopy (SEM) measurements were obtained using an Amray 1810 T microscope and atomic force microscopy (AFM) was carried out using a Digital Instruments Dimension 3100 microscope in tapping mode.

Devices were processed using 5 μm CdTe/2000 Å CdS/ITO/glass structures. The CdTe was deposited by vapor transport technique. All substrates received a post-deposition high-temperature anneal and $CdCl_2$ treatment. Contacts were completed by depositing 6% w/w Cu/graphite paste and annealed at 200°C in Ar(g) for 30 min.

THEORY

Ellipsometry measures the ratio of p-and s- (the electric fields parallel and perpendicular to the incident plane, respectively) complex reflectance of the sample. This is seen from the fundamental equation given by;

$$\tan \Psi e^{i\Delta} = \frac{R^p}{R^s}$$

where R^p and R^s are the total complex reflection coefficients for the p- and s-waves, respectively. The parameters Ψ and Δ, known as the ellipsometry parameters, correspond to the ratio of the magnitude of the total reflection coefficient and the phase shift in the p-and s-waves upon reflection, respectively. Ellipsometry measures Ψ and Δ for a material, from which optical constants, film thickness etc., can be extracted using optical models. The ellipsometry parameters are highly sensitive to the surface properties. In this paper, optical data is presented in terms of the imaginary part of the complex dielectric constant, ε_2. From the knowledge of the electronic transitions in different materials, one can qualitatively assign the peaks that consistently appear in the ε_2 spectra to materials within the sample. The observance of the peak and its position,

corresponding to an electronic transition, is largely depend on the quantity and quality of the material. Generally, NP etching generates sufficient Te to detect its characteristic peak at 2.1eV in the ε_2 spectra. On the other hand, BM etching generates less Te, and the 2.1 eV peak is not detectable. However, due to its high polarizabilty, the presence of even just a few Å of Te improves the overall dielectric response of the sample. We monitor this improvement by noting the changes in CdTe ε_2 peaks at 3.3 eV, the transition energy for E_1, and at 3.9 eV, the $E_1+\Delta_1$ transition [4]. The latter peak is very sensitive to the presence of native oxides, exhibiting a decrease in intensity with respect to the E_1 peak.

RESULTS AND DISCUSSION

Etching of CdTe

As NP1 etching proceeds, bubbles are observed on the CdTe surface after ~20 sec immersion [1]. The CdTe surface becomes silvery-gray and roughened. A thick and conductive Te layer is produced on CdTe with NP1 etching [1,5]. The time for the bubbles to appear can vary and is dependent on a number of conditions, including concentration, temperature, and the presence of oxides on the CdTe film. The acidity of the NP solution is expected to remove any CdTe- and Te- oxides formed during etching. No bubbling is observed during BM etching, but a polished Te-rich CdTe surface is typically formed [2,6].

Figure 1 shows ε_2 vs. photon energy plots obtained from VASE measurements of an unetched CdTe film and of films after receiving a 20 sec etch in NP1 and after a 10 sec etch in 0.1% BM. The ε_2 spectrum of the unetched film contains the two characteristic CdTe E_1 and $E_1+\Delta_1$ peaks [4]. Following etching in NP1, the spectrum now contains a single peak at 2.1 eV, due to Te [4]. The CdTe peaks are not detectable, indicating a high proportion of Te at the surface. The Te peak was observed to grow and sharpen with subsequent VASE scans before reaching a maximum intensity ~10 min after etching. These changes can be attributed to crystallization of the Te and this was confirmed using GIXRD. Figure 2 shows a series of GIXRD scans, recorded

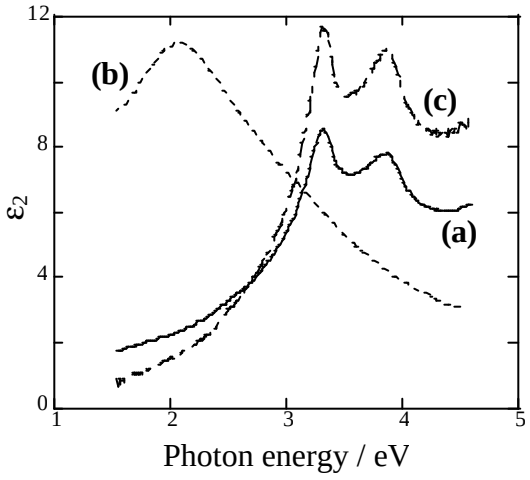

Figure 1. VASE ε_2 spectra of (a) an unetched CdTe film and CdTe films following etching in (b) NP1 for 20 sec and in (c) 0.1% BM for 10 sec.

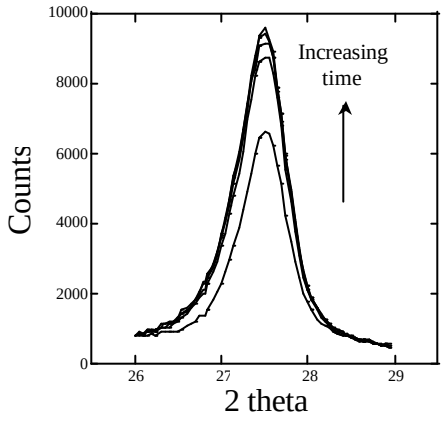

Figure 2. GIXRD patterns, obtained over time, of a CdTe film following a 25 sec NP1 etch. Incident angle was 2° and each scan cycle is ~3 min apart.

over time, of a CdTe film following etching in NP1 for 25 sec. Each scan cycle was ~3 mins apart. The Te (101) peak is observed to grow over time, completing crystallization ~10 min after etching. It was found that if CdTe is etched in NP1 for >40s, crystallization occurs during the etch and a ~100 nm crystalline-Te (c-Te) film is observed. Etching for <35 sec results in amorphous-Te (a-Te) films that spontaneously crystallize, observed with VASE and GIXRD, following removal from solution. Crystallization time increases for shorter etches, e.g. less than 5 min for a 35 sec etch to over 1 hr for a 15 sec etch. a-Te is known to be unstable at room temperature [1,7], due to its low glass-transition temperature, and spontaneously crystallizes. The slower crystallization with shorter etches can be attributed to the lesser amounts of generated a-Te. Because of the lower Te concentration, molecular rearrangements of Te crystallization will require a longer time to complete.

In contrast, BM etching of CdTe is known produce thin Te films of only a few angstroms thickness [6]. In figure 1c, the characteristic Te ε_2 peak is not observed in the spectrum after etching. However, an increase in the intensity of the CdTe spectrum is seen due to the smoother surface and increased dielectric response in the presence of Te. The ε_2 Te peak was not observed in the spectra for BM etching of up to 60 sec. Also, no c-Te was detected using GIXRD on any BM-etched CdTe. X-ray photoelectron spectroscopy has been previously used to confirm that a Te-rich surface is formed with BM etching of CdTe [2,3]. Modeling of the VASE ε_2 spectrum of BM etched CdTe in figure 1 suggests that a very thin, 7-8 Å, a-Te film is formed.

Oxidation of etched CdTe

Delays between etching and contacting are known to allow the formation of oxides on the freshly etched CdTe surfaces, which may affect back contact performance and reproducibility. The stability of etched CdTe towards oxidation was monitored using VASE. Freshly etched samples were placed on the VASE in ambient air and were measured over several hours. Figure 3 shows the amplitudes of the 2.1 eV and 3.3 eV photon energies obtained from ε_2 spectra of 25 sec NP1-etched and 60s 0.01% BM-etched CdTe films, respectively. The amplitudes for the first 100 min after etching are shown. These energies coincide with the Te peak and CdTe E_1 peaks, respectively (Figure 1). As no Te peak is detected with BM etching, the CdTe E_1 peak is profiled

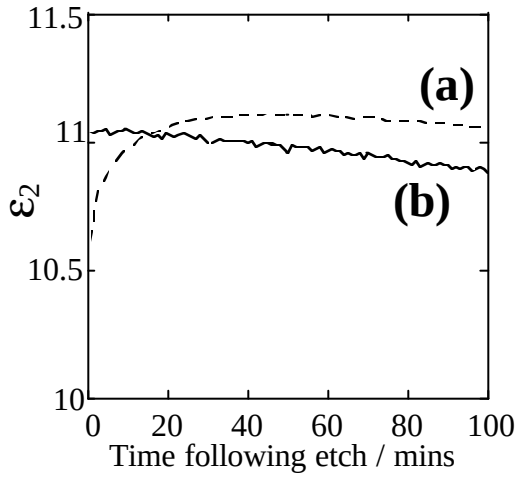

Figure 3. Time profiles of ε_2 from (a) 25 sec NP1 and (b) 60 sec 0.1% BM etched CdTe films. ε_2 values were obtained at 2.1 eV and 3.3 eV wavelengths, respectively.

as oxidation of the Te-rich surface will result in a decrease in dielectric response of the film and, hence, a decrease in spectral intensity.

Following the NP1 etch, a rapid increase in ε_2 intensity is observed due to Te crystallization. Following completion of crystallization, no changes are observed until ~60 mins, when the intensity begins to decrease as a result of atmospheric oxidation. This oxidation continues till around 7-8 hrs after etching. No oxidation was apparent on CdTe films that were stored in either vacuum or dry air immediately following etching, suggesting humidity plays a significant role

in air oxidation of Te. The BM etched film shows that air oxidation of the Te begins immediately following etching and continues for 3-6 hours. The fast oxidation of the BM etched surface can be attributed to the Te film being very thin and highly amorphous. These observations highlight the need for cells to be contacted immediately following etching.

Morphological effects of NP etching

In studies using NP etches of similar composition to NP1, etch times of ~60 sec are required to produce good-quality cells [5,8]. Such long NP etches result in significant widening of the GBs

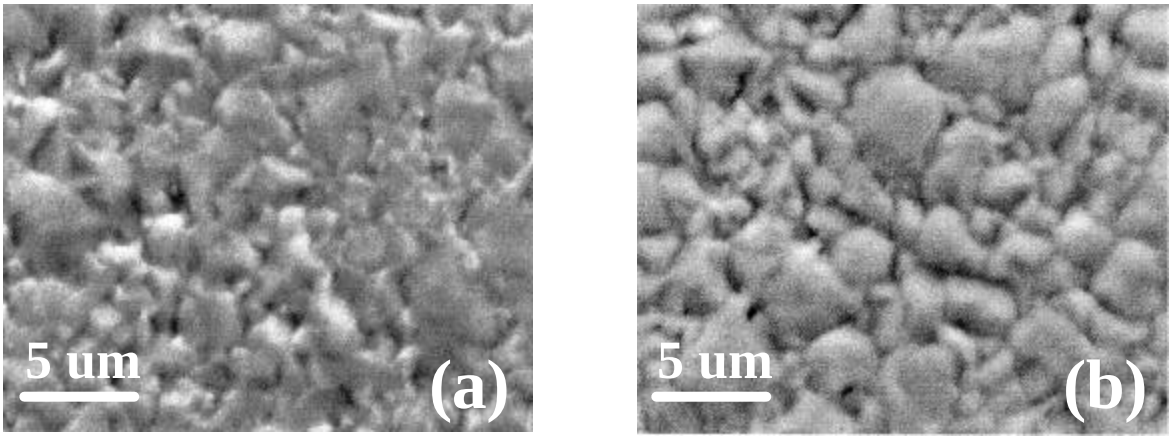

Figure 4. SEM images from a CdTe film (a) before and (b) after 60 sec NP1 etch.

[5,8]. Figure 4 shows SEM images of a CdTe film before and after etching in NP1 for 60 sec. It can be clearly seen the etch treatment significantly smoothes grain morphology and the GBs are now more prominent as a result of the treatment. It is expected that the GBs would contain a high degree of c-Te. SEM images of BM etched films show little apparent change in film morphology [8]. The significant GB etching that occurs during NP1 treatments indicates that NP etching may not be suitable for treatments of CdTe films of less than 5 μm thickness. Li *et al*. [5] have shown that GB etching of NP can extend a significant distance into the film. The authors pointed out that GB etching, leaving conductive Te-rich layers through the GBs, would alter the bulk properties of the films and could result in device shunting. Danaher *et al*. [2] have shown SIMS analysis of 3 μm CdTe/CdS/ITO/glass structures etched in 0.1% BM for 5 sec. High concentrations of Br were found through the CdTe layer, including an apparent accumulation of Br at the CdS/ITO interface. These observations raise a number of questions regarding the use of wet chemical etches; specifically regarding the rate of etchant penetration, the role of GB widening in the diffusion Cu, O and other impurities [8], and effects of changing GB integrity on device performance.

Alternate NP and Br_2 etches

The properties of the NP and BM etch solutions were adjusted in order to allow fast reaction with the CdTe surface while preventing GB penetration/etching and maintaining GB integrity. For NP, etches of higher acidity were considered. NP2 and NP3, containing 1% and 0.5% HNO_3 in H_3PO_4, respectively, were prepared without addition of H_2O. By increasing the acidity, a faster surface reaction is expected. This is confirmed by the almost instant appearance of bubbles during NP2 and NP3 etching of CdTe. Shorter etch times, therefore, should be required to generate sufficient Te and thus reducing the time available for GB penetration by the etchants. Increasing the concentration of H_3PO_4 also increases the viscosity of the solutions, which is expected to slow GB penetration. A series of Br_2 etches were prepared using alcohol solvents of varying viscosities. Again, this is expected to slow Br_2 GB penetration during etching.

Figure 5 shows sets of ε_2 VASE data of CdTe films obtained over time following etching in NP3

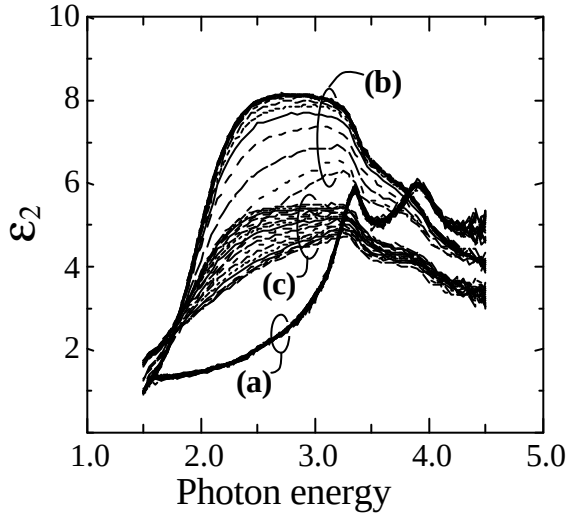

Figure 5. Sets of VASE ε_2 spectra obtained over time from CdTe films following (a) 2 sec, (b) 6 sec and (c) 8 sec etches in NP3.

for 2, 6 and 8 sec. Similar data was obtained for NP2, but with shorter etches. The 2 sec NP3 etch (the figure 5a set of spectra) shows no formation of Te. Longer etches produce a-Te on the CdTe surface, with a maximum amount produced with 4-6 sec immersion (figure 5b set). The a-Te is seen to crystallize over time, with growth of the Te ε_2 peak, following removal from the solution. Crystallization was complete within 20 mins. For NP2, maximum a-Te was produced

after just 2-4 sec. Etching for longer times results in a decrease in generated a-Te. NP3 etching for 8 sec results in a decrease in the Te peak (figure 5c set). This is due to either oxidation of the Te by the etch solution or the result GB etching forming significant voids in the film. Crystallization of the generated a-Te is still observed for the 8 sec etched film, though the process takes longer, ~30 min, to complete due to the lesser amount of Te formed. Unlike for NP1, significant CdTe peaks remain in the VASE spectra of the NP2 and NP3 etched samples, also indicating that less net Te is produced compared to NP1. SEM measurements show no significant changes in film or GB morphology after 4-6s etching in NP3, but GB etching is observed following etching for >8 sec.

A series of 0.1% Br_2 etches were prepared using a number of alcohol solvents of differing viscosities. Br_2 can react with alcohols, though the reaction with primary alcohols used in this study is sufficiently slow to not initially affect the strength of the etch solution. Some secondary alcohols, like isopropanol and cyclohexanol, were found to rapidly react with Br_2, decolorizing the solution within a few minutes. These solvents were not used for etching experiments. Table 1 shows a list of the solvents, with their viscosities, used to produce the Br_2 solutions. Figure 6 shows film surface roughness (R_{ms}), obtained from AFM images of 20 μm x 20 μm areas, of the CdTe films after 10 sec etches in the viscous Br_2 solutions, plotted against etch viscosity (η). The R_{ms} of a non-etched film is shown at η = 0 mPa s for comparison. The plot shows that the films are significantly etched in the lower η solvents, with smoothing of the surface by the polishing etch. The rate of surface polishing decreases with increasing η, and appears to become constant at approximately η=20 mPa s. For solvents of η>20 mPa s, generation of only very small amounts of surface-Te is observed. Etching in Br_2/glycerol (not shown) showed no effect on the CdTe surface.

For all Br_2 solutions, VASE ε_2 spectra showed generation of Te as a spectral intensity increase of the CdTe peaks, due to increased extent of polishing and formation of Te. The degree of increase in CdTe spectral intensity scaled with decreasing solvent η, confirming the AFM observations. We note that in figure 6, the point corresponding the Br_2/2-ethyl-1-hexanol etched sample lies off the data trend. From VASE measurements, however, this sample agreed with the observed trend. The discrepancy from the R_{ms} data is probably the result of sampling an unrepresentative area of the film surface.

Etching Mechanisms

The mechanisms of CdTe etching can be discerned from considering the general redox chemistry of the reactive species involved. However, this does not necessarily give an accurate appreciation of the chemical dynamics occurring both at the surface and in the solution during etching. To attempt to discern the various processes occurring during etching, a number experiments were carried out to evaluate the chemistry of CdTe.

Table 1 – Viscosity of solvents used for Br_2 etching [9]. Water is included for comparison.

Solvent	η (25°C) /mPa s
methanol	0.5
water	0.9
1-butanol	2.5
2-ethyl-1-hexanol	6.3
1-decanol	10.9
ethylene glycol	16.1
diethylene glycol	30.2
glycerol	930

Treating CdTe films with just concentrated H_3PO_4 or 1% HNO_3 in H_2O resulted in only the removal of oxides on the CdTe film. This was observed using VASE from growth of the $E_1+\Delta_1$ CdTe peak. No Te was formed with either of these solutions.

Using the appearance of bubbles as a reference, the effect of incremental NP1 etches on the same sample was investigated using VASE. Two similar experiments were carried out, where single samples were etched in 20 sec steps, i.e. prior to bubbling, and in 30 sec steps. Figure 7 shows the profile of the intensity of the 2.1 eV Te peak in ε_2 spectra as a function of total etch time. Crystallization of a-Te was allowed to complete before data was obtained. The sample receiving 30 sec etches shows fast formation of Te, reaching a maximum following just two treatments. A steady decrease in the amount of Te was observed with each subsequent etch, while time for bubbles to appear decreased to 16 – 18 sec. The film receiving 20 sec etches shows a slow formation of Te, requiring around 8 treatments to reach a maximum amount of Te. With subsequent treatments, the level of Te remained constant, indicating saturation of the CdTe surface had occurred. A 30 sec etch was then carried out on the sample, which resulted in an immediate decrease in Te, and continued to decrease with subsequent 30 sec etches. Finally, a series of 10 sec etches were carried out and consumption of Te ceased. These observations suggest that significant formation of Te occurs during the initial stages of etching, but occurs

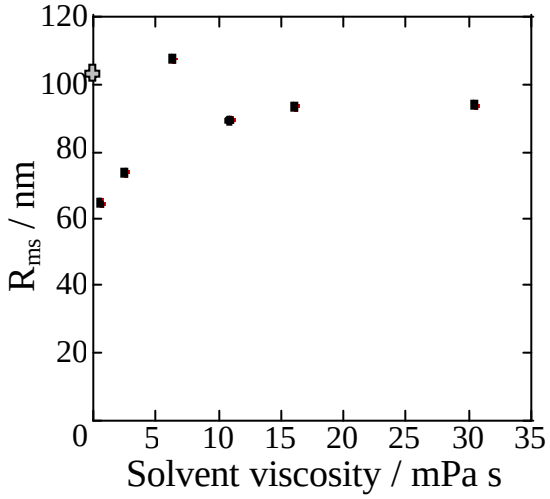

Figure 6. Plot of R_{ms}, obtained from AFM, vs. etch solution viscosity for CdTe films etched with viscous Br_2 solutions (dots). Unetched CdTe is plotted at η=0 mPa s for comparison (cross).

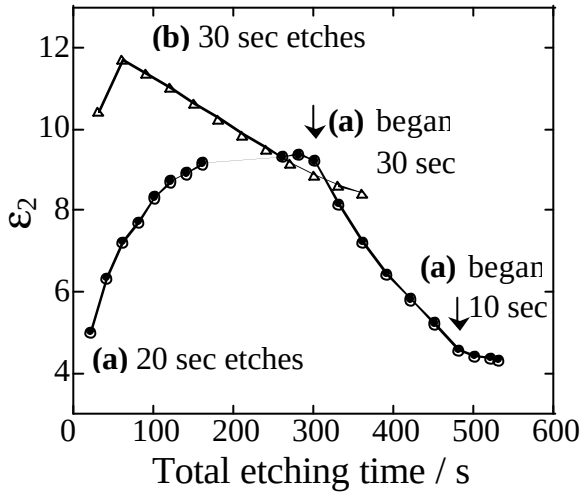

Figure 7. Profile of the ε_2 intensity of the 2.1 eV Te peak following etching of CdTe films for a series of (a) 20 sec and (b) 30 sec subsequent treatments in NP1. For plot (a), the CdTe film also received a number of subsequent 30 sec and 10 sec NP1 etches, which are highlighted.

more rapidly after bubbling. This may be explained by oxidation of Te and/or GB etching, which appear to only occur after bubbling and suggests that this reaction proceeds rapidly enough to allow nucleation of bubbles of the gaseous side-product. Until saturation, oxidation of Te^{2-} to Te appears to be the dominant reaction.

A series of test-tube reactions were carried out to observe the general chemistry of the NP1 and NP2 etches with CdTe and Te crystals. The CdTe crystals reacted with both NP etches, showing rapid bubbling on the CdTe surface and the formation of brown NO_2 gas above the solution. With NP2, the solution became a yellow-green color for ~1 day before fading, however, no color change was observed with NP1. Both reactions were complete after a few days, leaving a black solid residue. When Te crystals were reacted with NP2, bubbling was observed with the formation of NO_2 gas and the solution color change, indicating that a Te species is responsible for the solution color. All the Te dissolved in the NP2 solution, but a white TeO_2 powder precipitate was observed after a few days.

These observations confirm that the bubbles formed during etching are due to production of NO_2(g) or NO(g). Note that NO(g) rapidly converts to NO_2(g) on reaction with air. The action of H_3PO_4 and 1% HNO_3 solutions on CdTe, resulting in only the removal of oxides, indicates that the NP etch relies on the oxidizing power of HNO_3 in the presence of excess H^+ ions, which are supplied by H_3PO_4. We note from the half-cell reaction for NO_3^- reduction;

$$NO_3^- + 4H^+ + 3e \rightarrow NO + 2H_2O$$

that 4 H^+ ions are required for each NO_3^- ion. HNO_3 alone supplies only 1 H^+ per NO_3^- ion. As H_3PO_4 is also unreactive towards CdTe, it is a suitable choice of acid. The addition of H_2O in NP1 appears to be only to dilute the solution to slow the overall rate of reaction.

The rapid reaction of Te in concentrated HNO_3 is well known, forming the yellow $Te^{4+}(aq)$ ion that is also formed during NP2 etching of CdTe crystals. The absence of the color change with NP1 etching suggests the higher acidity solutions allow a different CdTe etch mechanism. The Pourbaix diagram for Te in aqueous systems [10] shows that oxidizing Te at pH < -1 results in the formation of $Te^{4+}(aq)$, while carrying out the reaction at slightly higher pHs allows the production of TeO_2. TeO_2 is expected to dissolve in the acidic solution to form solvated Te-oxides, e.g. $HTeO_2^+$. The absence of the yellow color during reaction of CdTe crystals with NP1 suggests that the latter mechanism is occurring. The direct oxidation of Te to $Te^{4+}(aq)$ with NP2 is expected to be a fast process compared to formation and dissolution of TeO_2, and would result in an oxide free surface. Undissolved residual oxides, expected following NP1 etching, could affect back contact quality.

For Br_2 etching, Br_2 is a relatively strong oxidizing agent and is expected to easily convert CdTe to Te. The generated Te also reacts with Br_2. 5 μm thick Te films begin to dissolve in 0.05% BM after 20 sec immersion. This reaction may be of a similar rate to CdTe etching and may account for why only very thin Te surface films are produced in BM.

Device analysis

Preliminary device analysis comparing the NP and Br_2 etch treatments for contact processing has been carried out. Initially devices were prepared by evaporating ~10 nm of Cu onto the etched surface, annealing and completing with graphite paste. However, this resulted in a high degree of shunting for cells with thin Te surface films. To avoid this, cells were completed by coating the etched CdTe with graphite paste containing 6% w/w Cu powder and annealing. Most of the completed devices, independent of etch, showed similar J-V characteristics; V_{oc} ~700 mV, J_{sc} ~ 15 mA cm^{-2} and FF ~55-60% and efficiencies ~ 6-6.5%. We note that the back contacts were not optimized for the substrate or each etch treatment. Generally, it is observed that for NP etching, the best performing cells are obtained from etch treatments which produce the most Te. For NP1 etching, this is generally occurred for etches of 30-60 sec, while for NP2 and NP3, the best cells were obtained following with 2 and 6 sec etches, respectively. These cells exhibited the highest J_{sc} and V_{oc} and lowest series resistance (R_s).

Some NP etched devices have received preliminary stress testing. A series of CdTe/CdS devices were processed following NP1 etching for 20, 30, 45 and 60s, and one device received a 20s 0.05% BM etch. Devices were stressed in air at 85°C in the dark. Figure 8 shows the plot of R_s of the devices before and after stressing with etching time. R_s was similar for each device prior to stressing, though slightly higher for devices that received shorter etches. During 30-40 days stress, very little degradation occurred in any of the cells. Following 55 days stress, some degradation was observed in the devices that had received shorter etches. No V_{oc} or J_{sc} losses or forward-bias rollover was observed for any of the devices. The degradation observed for the short etched cells is due to increases in R_s (figure 8). The 60 sec NP etched device shows only a very slight R_s increase. The BM-etched device exhibited a significant increase in R_s, though less than that observed for the 20 sec NP-etched sample. This suggests back contacts with high Te content may exhibit improved performance and stability.

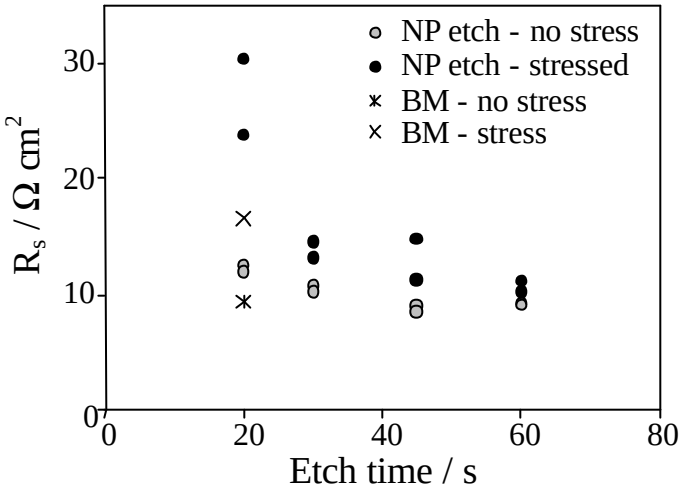

Figure 8. Plot of R_s, before and after stressing at 85°C in air and in the dark, vs. etch time for devices that received NP1 etching during back contact processing. R_s values, before and after stress, for a device etched in 0.05% BM are also shown. Two cells were prepared on each device.

Some devices have also been prepared by etching for 20 sec in 0.05% Br_2 solutions of differing viscosities. Initially, all devices showed photovoltaic behavior, however, after ~12 hrs, the devices etched in solutions of η>20 mPa s were found to have become highly shunted or completely shorted. This highlights the fast diffusion kinetics of Cu, most likely via GBs, in CdTe films. The J-V characteristics of the other devices were unchanged. Following thermal stressing for 55 days, the remaining devices exhibited degradation due to increases in R_s. However, the devices etched in Br_2\1-butanol and Br_2\ethylene glycol exhibited significantly greater R_s increases compared to devices etched in BM.

Back contact considerations

The action of NP etches on CdTe produces Te-rich films of up to ~100 nm thickness. The GB etching that occurs with longer NP etches may assist the penetration of Cu and other impurities throughout the device. However, the device stability results indicate that the mild degradation observed in this study was due to back contact effects and only occurred in the cells that received shorter etches. During the contacting processing, the Cu reacts with Te to produce a favorable back contact. During stress, the Cu is thought to diffuse into the device, eventually exhausting the back contact or poisoning the cell junction [11]. However, if the contact contains a thick Te film, coupled with the affinity of Cu for Te, the release of Cu into the CdTe will be significantly hindered. The thicker Te getters the Cu and maintains a favorable copper telluride back contact for a longer time. This is consistent with the R_s increases observed for cells processed with short NP1 or Br_2 etches, while no change in R_s was observed for cells that received longer NP1 etches. This suggests that a high Te content could allow the formation of back contacts of improved quality and stability to CdTe devices.

CONCLUSIONS

Etching of CdTe with NP and Br_2 solutions was monitored using VASE and GIXRD. Etching with NP was found to result in the formation of a-Te, which spontaneously crystallizes. NP1 etched surfaces were found to be stable to atmospheric oxidation for ~60 mins after etching, however, BM-etched surfaces begin to oxidize immediately. NP solutions of higher acidity rapidly etch CdTe, producing significant surface Te without GB etching. Increasing solution viscosity was shown to slow the rate of reaction of Br_2 with CdTe surfaces. Mechanistic considerations suggested that etching with higher acidity NP solutions proceeded via a different mechanism. Device analysis showed that devices that received longer NP1 etches during contacting exhibited no R_s increase during stress, suggesting that thicker Te films attenuate Cu diffusion into the CdTe layer and may allow the formation of better quality back contacts.

ACKNOWLEDGEMENTS

We acknowledge the support of the NREL Thin-Film Partnership, contract no. ADJ-1-30630-12. We thank S. Fields for CdTe depositions, V. DiNetta for AFM measurements and R. Dozier for J-V measurements.

REFERENCES

[1] J. Sarlund, M. Ritala, M. Leskela, E. Siponmaa and R. Zilliacus, *Sol. Energy Mater. Sol. Cells*, **44**, 177 (1996).
[2] W. J. Danaher, L. E. Lyons, M. Marychurch and G. C. Morris, Appl. Surf. Sci., **27**, 338 (1986).
[3] J.-P. Haring, J. G. Werthen and R. H. Bube, *J. Vac. Sci. Technol. A*, **1**, 1469 (1983).
[4] H. Arwin, D. E. Aspnes and D. R. Rhiger, *J. Appl. Physl.*, **54**, 7132 (1984).
[5] X. Li, D. W. Niles, F. S. Hasoon, R. J. Matson and P. Sheldon, *J. Vac. Sci. Technol. A*, **17**, 805 (1999).
[6] D. E. Aspnes and H. Arwin, *J. Vac. Sci. Technol. A*, **2**, 1309 (1984).
[7] W. Y. Lee, H. Coufal, C. R. Davis, V. Jipson, G. Lim, W. Parrish, F. Sequeda, and R. E. Davis, *J. Vac. Sci. Technol. A*, **4**, 2988 (1986).
[8] D. L. Batzner, R. Wendt, A. Romeo, H. Zogg, A. N. Tiwari, *Thin Solid Films*, **361**, 463 (2000).
[9] CRC Handbook of Chemistry and Physics, 70th ed., edited by R. C. Weast and M. J. Astle (CRC Press, Boca Raton, FL, 1989).
[10] M. Pourbaix, *Atlas of Electrochemical Equilibria in Aqueous Solutions* (Pergamon Press, Oxford, 1966).
[11] K. D. Dobson, I. Visoly-Fisher, G. Hodes and D. Cahen, *Sol. Energy Mater. Sol. Cells*, **62**, 295 (2000).